von Gastrow, Guillaume; Calle, Eric; Ortega, Pablo; Alcubilla, Ramon; Daniil, Andreana ; Stutz, Elias Z.; Fontcuberta i Morral, Anna; Husein, Sebastian; Nietzold, Tara; Bertoni, Mariana; Savin, Hele

Metallized Boron-Doped Black Silicon Emitters For Front Contact Solar Cells

Published in:
2017 IEEE 44th Photovoltaic Specialists Conference (PVSC)

DOI:
10.1109/PVSC.2017.8366010

Published: 01/01/2018

Document Version
Peer reviewed version

Metallized Boron-Doped Black Silicon Emitters For Front Contact Solar Cells

Guillaume von Gastrow[1], Eric Calle[2], Pablo Ortega[2], Ramón Alcubilla[2], Andreana Daniil[3], Elias Z. Stutz[3], Anna Fontcuberta i Morral[3], Sebastian Husein[4], Tara Nietzold[4], Mariana Bertoni[4], and Hele Savin[1]

[1]Aalto University, Espoo, 02150, Finland
[2]Universitat Politècnica de Catalunya, Barcelona, 08034, Spain
[3]École Polytechnique Fédérale de Lausanne (EPFL), Lausanne, 1015, Switzerland
[4]Arizona State University, Tempe, Arizona, 85287, USA

***Abstract* — We study doping and metallization of black silicon (bSi) boron emitters formed by ion implantation or diffusion. We demonstrate that conformal metal layers can be deposited on bSi by electron beam evaporation. Raman spectroscopy shows that high boron concentrations ($4 \cdot 10^{19}$ cm^{-3}) are obtained in bSi by ion implantation, while maintaining emitter saturation current (J_{0e}) below 20 fA/cm^2 with Al_2O_3 passivation. In diffused bSi emitters, doping increases to twice the values of planar substrates, reaching values up to $7 \cdot 10^{20}$ cm^{-3}. Those doping values allow specific contact resistivities down to (0.3 ± 0.2) mΩ·cm^2 on boron-implanted bSi surfaces with nickel or aluminum contacts.**

***Index Terms* — black silicon, contact resistance, emitter, doping**

I. Introduction

Silicon solar cell surface nanostructures – also called black silicon, or bSi – provide a definite advantage in terms of reflectance reduction [1]. The efficiency of bSi front-side emitter solar cells remains however poor due to three main issues: 1) the high recombination due to large surface area [2], 2) the high Auger recombination caused by heavy diffusion of dopants [3], and 3) the lack of conformality of metal contacts due to the high aspect ratio of the structures [4]. While the surface recombination issue can be solved by ALD Al_2O_3 passivation [5, 6], the two others still remain recurrent issues with the standard emitter formation techniques. However, alternative methods exist and could allow the fabrication of performant bSi emitters without modification of the nanostructures. For instance, ion implantation is a promising doping technique for bSi, as it uses a fixed dopant dose and thus allows better doping control than diffusion in bSi structures, causing less recombination [7]. Electron beam evaporation could constitute a solution for contact formation, as it allows low deposition rates to produce conformal layers [8] and ensures limited surface damage [9]. Here we study whether ion implantation and electron beam evaporation can be combined to fabricate metallized bSi emitters with limited recombination activity and low contact resistance. In addition, doping is an important parameter to consider when optimizing emitter passivation and metallization, but it is typically difficult to measure in bSi structures. Successful silicon nanowire doping measurements have been performed by CV measurements [10], although they remain complex due to the need for maintaining a contact with the nanowires. In this work, we utilize Raman spectroscopy, which has the advantage of being a contactless method. The first part of this paper focuses on doping mechanisms in bSi structures and the second one on contact performance.

II. Experimental Details

The substrates were (100)-oriented magnetic Czochralski phosphorus-doped silicon wafers with a resistivity of 3.4 Ohm·cm and a thickness of 445 µm. Black silicon was produced by inductively-coupled reactive ion etching in a SF_6/O_2 plasma at a temperature of -120 °C. Boron implantation was performed at an energy of 10 keV and with a dose of $3 \cdot 10^{15}$ cm^{-2}. Then, a 20 min anneal was performed in N_2 ambient at temperatures of 950 °C and 1050 °C, followed by dry oxidation for 20 min at the same temperatures. Boron diffusions were performed at temperatures of 825 °C and 975 °C for 45 min with a solid source. The samples were then dipped in a 5 % HF solution for two minutes. The boron-rich layer was etched with low thermal oxidation (LTO) in pure O_2 atmosphere at 650 °C for 30 min, followed by another 5 % HF dip for 2 minutes. In addition, planar reference wafers were implanted and diffused using the same parameters.

Nickel contacts with thicknesses ranging from 100 nm to 400 nm were formed by e-beam evaporation at a rate of 0.1 nm/s and at an initial pressure of $6 \cdot 10^{-7}$ mbar. The rate was increased to 0.5 nm/s after a thickness of 200 nm was reached. Aluminum contacts of 1 µm were also deposited with e-beam evaporation at an initial rate of 0.1 nm/s and annealed in forming gas at 400 °C for 10 minutes. The nickel-coated samples were measured before and after post-deposition anneal. Annealing was performed at temperatures from 350 °C to 450 °C during 30 seconds to three minutes in N_2 ambient or in forming gas. Specific contact resistivity was measured with the transfer length method.

Raman spectroscopy measurements were performed at wavelengths of 405 nm and 532 nm, corresponding

approximately to an absorption depth of 100 nm and 1 µm in planar silicon, respectively.

III. Emitter Doping

Excellent passivation results have been obtained in our previous study with atomic layer deposited Al_2O_3 on implanted bSi emitters annealed at 1000 °C and 1050 °C. An emitter saturation current (J_{0e}) of 20 fA/cm^2 was reported at both temperatures. Reasonably low J_{0e} of 30 fA/cm^2 and 110 fA/cm^2 were measured in emitters diffused at 825 °C and 975 °C, respectively [7]. Although this shows potential for integration in front-side-emitter solar cells, it is essential to determine whether such emitters also allow low-resistance contacts.

The corresponding sheet resistance values are summarized in Table I. In diffused emitters, doping increases with temperature, and consequently sheet resistance decreases. In implanted emitters however, the dopant dose is fixed, and sheet resistance remains stable once all dopants have been activated.

TABLE I
Sheet Resistance of Planar and Black Silicon Samples

Emitter formation	Sheet resistance (Ohm/sq)	
	planar	bSi
Diffusion, 825 °C	384 ± 1	260 ± 20
Diffusion, 975 °C	38 ± 2	21 ± 1
Implantation 950 °C	60 ± 1	200 ± 20
Implantation,1050 °C	56 ± 1	170 ± 5

Sheet resistance provides information on doping, which eventually indicates the potential for ohmic contact formation, but it remains unclear whether measurements on planar Si and on bSi are comparable. Additionally, doping can be measured by electrochemical capacitance voltage on planar samples (Fig. 1), but measurements on bSi become complex and unreliable.

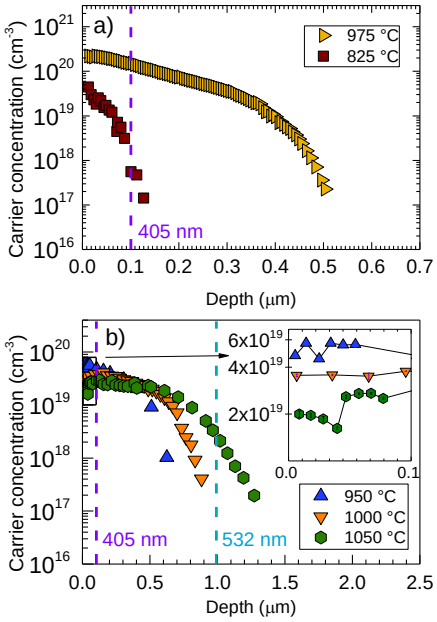

Fig. 1. Doping profiles measured by electrochemical capacitance voltage of a) boron-diffused emitters on planar samples at temperatures of 825 °C and 975 °C b) boron-implanted emitters on planar samples after annealing at 950 °C and 1050 °C. The dash lines indicate the absorption depth in silicon at wavelengths of 405 nm and 532 nm.

On the other hand, Raman spectroscopy is a contactless method that may help assessing the doping of bSi more accurately and allow comparison with planar samples. Examples of Raman spectroscopy measurements are shown in Fig. 2. The broadening and asymmetry of the Si TO-LO Raman peak can be related to the effective hole concentration via the Fano effect [11].

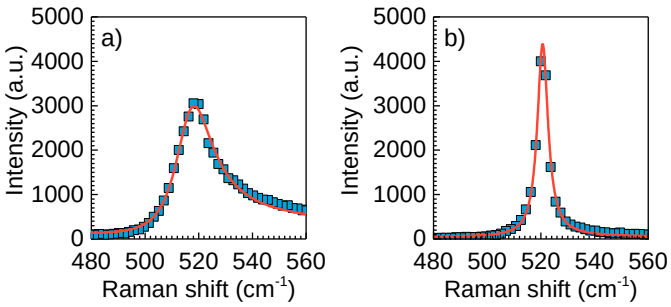

Fig. 2. Example of Raman spectroscopy measurements on a) a bSi sample diffused at 975 °C and b) a planar sample diffused at 975 °C. The Fano fits are indicated by red lines.

As an optical method, Raman spectroscopy can only assess the carrier concentration within the absorption length of the excitation wavelength λ_{exc} used. For λ_{exc} = 405 nm, this corresponds approximately to 100 nm. The results reported are thus effective carrier concentrations, which are convoluted along the whole corresponding absorption depth. In the case of bSi, one expects light to be confined at the surface. Raman spectroscopy provides information on the carrier concentration much closer to the surface than in the case of planar substrates and well below the absorption length of silicon. The effective hole concentrations obtained by Raman spectroscopy at different wavelengths are summarized in Fig. 3.

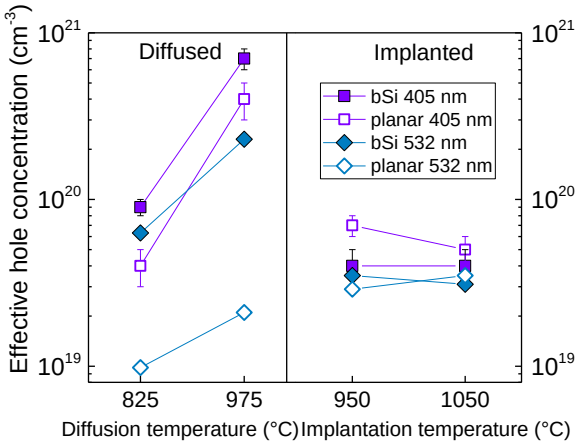

Fig. 3. Effective hole concentrations measured by Raman spectroscopy in diffused and in implanted emitters. Measurements were performed at wavelengths of 405 nm and 532 nm. The concentrations are effective values over the whole absorption depth, which corresponds to approximately 100 nm at a wavelength of 405 nm and 1 µm at a wavelength of 532 nm for planar silicon.

Relatively high hole concentrations – that reflect doping concentrations – are measured in all bSi emitters, which should thus allow performant electrical contacts [12]. The doping concentration measured in diffused bSi emitters is up to one order of magnitude higher than in the implanted emitters.

In diffused emitters, the comparison between the two excitation wavelengths indicates that doping at the surface (λ_{exc} = 405 nm) is higher than doping deeper in the bulk (λ_{exc} = 532 nm) for both bSi and planar substrates. At a wavelength of 532 nm, regions of low doping are also probed during the measurement, which is consistent with the low effective hole concentration obtained compared to the measurement performed at 405 nm. In addition, the diffused bSi samples seem to exhibit higher carrier concentrations than their planar reference at any given diffusion temperature.

Similarly in bSi implanted emitters, high hole concentrations over $3 \cdot 10^{19}$ cm^{-3} are detected. No clear variation in the hole density is observed between bSi samples and their planar reference or depending on implantation anneal temperature. This is consistent with the fixed nature of the implantation dose.

IV. Metallization And Contact Resistance

The doping and hole densities reported in section III suggest that performant contacts could be obtained on bSi diffused and implanted emitters. The following section studies the conformality and specific contact resistivity of nickel (Ni) and aluminum (Al) contacts and bSi. Nickel has a potential for excellent adhesion and for low contact resistance on silicon, acts as a copper barrier layer, and serves as a seed layer for copper electroplating [13]. In addition, aluminum contacts were also fabricated.

Fig. 4 shows that electron-beam evaporation allows conformal coating of bSi; 250 nm of Ni deposited by electron beam evaporation are sufficient to fully cover the structures.

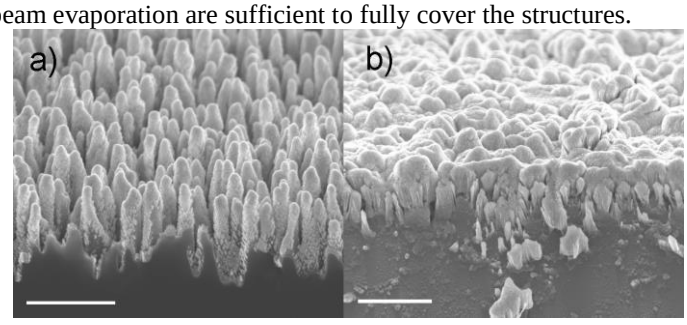

Fig. 4. SEM images of bSi structures metallized by electron gun evaporation with a) 100 nm of nickel and b) 250 nm of nickel. The scale bars represent 1 µm.

Nickel can provide a low contact resistance on silicon after formation of a silicide layer whose characteristics depend on the temperature [14]. The NiSi phase is thought to provide the lowest resistivity [15] and is usually obtained at very shorts anneals (from 30 seconds to 3 minutes) in a temperature range of 300 °C – 450 °C [16]. In this work however, post-deposition annealing did not seem to improve the contact resistivity of nickel. Fig. 5 displays the specific contact resistivity ρ_c in the different bSi emitters depending on the diffusion or implantation anneal temperature. The Ni samples were measured without post-deposition anneal, except for one set, which underwent annealing for 3 min at 400°C, as reported on the graph. It appears that excellent values down to 0.3 $m\Omega \cdot cm^2$ are obtained with Ni contacts on bSi without post-deposition annealing. It is possible that Ni annealing occured already during the evaporation process that caused severe heating of the samples for a long duration.

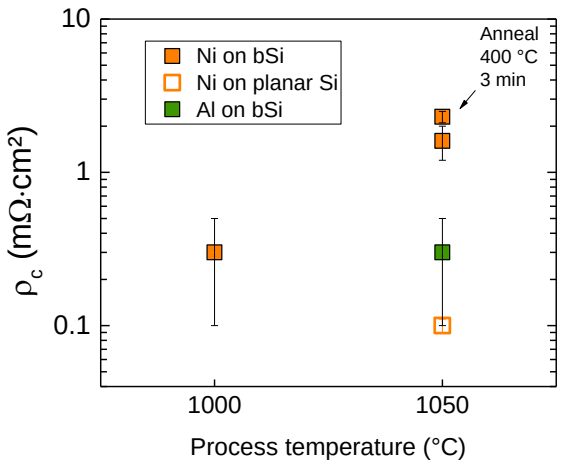

Fig. 5. Specific contact resistivity ρ_c measured in implanted bSi emitters at different implantation anneal temperatures. The results on Ni samples are reported without post-deposition annealing unless otherwise indicated. The Al sample was annealed at 400 °C for 10 min.

The implantation anneal temperature seems to affect the specific contact resistivity, possibly through surface doping. Although Raman measurements in Fig. 3 indicate a similar effective doping in the first 100 nm at the surface after implantation anneal at 1000 °C and 1050 °C, it is likely that the higher annealing temperature of 1050 °C reduces surface doping, thus causing high contact resistance. The value of 1 to 3 $m\Omega \cdot cm^2$ obtained with nickel after implantation anneal at 1050 °C can however be reduced to 0.3 $m\Omega \cdot cm^2$ with Al contacts. Measurements on planar reference samples implanted and annealed at 1050 °C indicate a very low specific contact resistivity compared to bSi samples. This may be explained by the high aspect ratio of bSi structures, causing shadowing and thus lower doping or no doping at all in some of the grooves between the spikes.

In diffused emitters, measurements were performed with a different set of structures that caued higher uncertainty. Thus, the specific contact resistivities measured ranged between 0,1 $m\Omega \cdot cm^2$ and 10 $m\Omega \cdot cm^2$.

V. Conclusions

We studied doping and contact formation bSi emitters. In bSi diffused emitters, the hole concentration near the surface was twice as high as in the planar references due to enhanced diffusion. In implanted emitters, an effective near-surface hole concentration of $(4 \pm 1) \cdot 10^{19}$ cm^{-3} was found both in planar and bSi samples. Consistent with these values, we reported excellent specific contact resistivities between 0.1 $m\Omega \cdot cm^2$ and 10 $m\Omega \cdot cm^2$ on black silicon emitters doped by boron implantation and by boron diffusion. Those emitters can also be efficiently passivated by ALD Al_2O_3 and display low emitter saturation current, as shown in our previous study. Consequently, both implanted and diffused black silicon emitters offer promising perspectives for solar cell applications.

Acknowledgements

This research was undertaken at the Micronova Nanofabrication Centre of Aalto University and in the cleanroom laboratory of the Micro and Nanotechnologies group at the Universitat Politècnica de Catalunya (UPC), Barcelona. This work was supported by the Spanish Ministry of Economy and Competitiveness MINECO (PCIN-2014-055) and Finnish TEKES (40329/14) agencies under Solar-Era.Net FP7 European Network. The work was also funded by the doctoral school of Aalto School of Electrical Engineering and the Project No. ENE2013-49984-EXP of the Spanish Ministry of Economy and Competitiveness (MINECO). AD, EZS and AFiM thank funding through the SNF Consolidator Grant 'Easeh'.

References

[1] P. B. Clapham and M. C. Hutley, "Reduction of Lens Reflexion by the "Moth Eye" Principle," Nature, vol. 244, pp. 281-282, 08/03, 1973.

[2] J. Oh, H. Yuan and H. M. Branz, "An 18.2%-efficient black-silicon solar cell achieved through control of carrier recombination in nanostructures," Nat Nano, vol. 7, pp. 743-748, print, 2012.

[3] S. Jeong, M. D. McGehee and Y. Cui, "All-back-contact ultra-thin silicon nanocone solar cells with 13.7% power conversion efficiency," Nat Commun, vol. 4, 12/16, 2013.

[4] S. Wang, Q. Li, K. Tao, R. Jia, S. Jiang, D. Wang and H. Dong, "Effective way to realize optimized carrier recombination and electrode contact for excellent electrical performance silicon nanostructure based solar cells," J. Mater. Sci. : Mater. Electron., vol. 27, pp. 4378-4384, 2016.

[5] M. Otto, M. Kroll, T. Käsebier, R. Salzer, A. Tünnermann and R. B. Wehrspohn. Extremely low surface recombination velocities in black silicon passivated by atomic layer deposition. Appl. Phys. Lett. 100(19), 2012.

[6] P. Repo, A. Haarahiltunen, L. Sainiemi, M. Yli-Koski, H. Talvitie, M. C. Schubert and H. Savin, "Effective Passivation of Black Silicon Surfaces by Atomic Layer Deposition," IEEE Journal of Photovoltaics, vol. 3, pp. 90-94, 2013.

[7] G. von Gastrow, P. Ortega, R. Alcubilla, S. Husein, T. Nietzold, M. Bertoni and H. Savin, "Recombination processes in passivated boron-implanted black silicon emitters," J. Appl. Phys., vol. 121, pp. 185706, 2017.

[8] J. Singh and D. Wolfe, "Review Nano and macro-structured component fabrication by electron beam-physical vapor deposition (EB-PVD)," J. Mater. Sci., vol. 40, pp. 1-26, 2005.

[9] A. Kuroyanagi, "Properties of aluminum-doped ZnO thin films grown by electron beam evaporation," Japanese Journal of Applied Physics, vol. 28, pp. 219, 1989.

[10] E. C. Garnett, Y. Tseng, D. R. Khanal, J. Wu, J. Bokor and P. Yang, "Dopant profiling and surface analysis of silicon nanowires using capacitance–voltage measurements," Nature Nanotechnology, vol. 4, pp. 311-314, 2009.

[11] B. G. Burke, J. Chan, K. A. Williams, Z. Wu, A. A. Puretzky and D. B. Geohegan, "Raman study of Fano interference in p - type doped silicon," J. Raman Spectrosc., vol. 41, pp. 1759-1764, 2010.

[12] R. Müller, J. Benick, N. Bateman, J. Schön, C. Reichel, A. Richter, M. Hermle and S. W. Glunz, "Evaluation of implantation annealing for highly-doped selective boron emitters suitable for screen-printed contacts," Solar Energy Mater. Solar Cells, vol. 120, Part A, pp. 431-435, 1, 2014.

[13] A. Mondon, M. Jawaid, J. Bartsch, M. Glatthaar and S. Glunz, "Microstructure analysis of the interface situation and adhesion of thermally formed nickel silicide for plated nickel–copper contacts on silicon solar cells," Solar Energy Mater. Solar Cells, vol. 117, pp. 209-213, 2013.

[14] J. D. Lee, H. Y. Kwon and S. H. Lee, "Analysis of front metal contact for plated Ni/Cu silicon solar cell," Electronic Materials Letters, vol. 7, pp. 349-352, 2011.

[15] V. Teodorescu, L. Nistor, H. Bender, A. Steegen, A. Lauwers, K. Maex and J. Van Landuyt, "In situ transmission electron microscopy study of Ni silicide phases formed on (001) Si active lines," J. Appl. Phys., vol. 90, pp. 167-174, 2001.

[16] T. Ohguro, S. Nakamura, M. Koike, T. Morimoto, A. Nishiyama, Y. Ushiku, T. Yoshitomi, M. Ono, M. Saito and H. Iwai, "Analysis of resistance behavior in Ti-and Ni-salicided polysilicon films," IEEE Trans. Electron Devices, vol. 41, pp. 2305-2317, 1994.